# Paper 7

# The detection and location of low magnitude earthquakes in northern Norway using multi-channel waveform correlation

**Gibbons, S.J., Sørensen, M.B., Harris, D.B. and Ringdal, F.**

**Submitted to Physics of the Earth and Planetary Interiors**

# The detection and location of low magnitude earthquakes in northern Norway using multi-channel waveform correlation at regional distances

Steven J. Gibbons [a] Mathilde Bøttger Sørensen [b]
David B. Harris [c] Frode Ringdal [a]

[a] *NORSAR, P.O. Box 53, N-2027 Kjeller, Norway.*

[b] *Department of Earth Sciences, University of Bergen, Allegt. 41, N-5007 Bergen, Norway.*

[c] *Lawrence Livermore National Laboratory, P.O. Box 808, Livermore, CA 94550, USA.*

**Abstract**

A fortuitous sequence of closely spaced earthquakes in the Rana region of northern Norway, during 2005, has provided an ideal natural laboratory for investigating event detectability using waveform correlation over networks and arrays at regional distances. A small number of events between magnitude 2.0 and 3.5 were recorded with a high SNR by the Fennoscandian IMS seismic arrays at distances over 600 km and three of these events, including the largest on June 24, displayed remarkable waveform similarity even at relatively high frequencies. In an effort to detect occurrences of smaller earthquakes in the immediate geographical vicinity of the June 24 event, a multi-channel correlation detector for the NORSAR array was run for the whole calender year 2005 using the signal from the master event as a template. A total of 32 detections were made and all but two of these coincided with independent correlation detections using the other Nordic IMS array stations; very few correspond to signals detectable using traditional energy detectors. Permanent and temporary stations of the Norwegian National Seismic Network (NNSN) at far closer epicentral distances have confirmed that all but one of the correlation detections at NORSAR in fact correspond to real events. The closest stations at distances of approximately 10 km can confirm that the smallest of these events have magnitudes down to 0.5 which represents a detection threshold reduction of over 1.5 for the large-aperture NORSAR array and over 1.0 for the almost equidistant regional ARCES array. We have applied the double-difference algorithm to relocate the events under various scenarios, but the incompleteness of the local network recordings precludes a comprehensive double-difference location for the full set of events. We note however that, where sufficient local network data exists, differential S-P travel times observed from stations at different azimuths suggest that

the hypocentral separation does not exceed 0.5 km in any given direction. Clear peaks were observed in the NORSAR correlation coefficient traces during the coda of some of the larger events; the local stations confirm that these are in fact aftershocks exhibiting very similar waveforms to the main events. Many of the more marginal correlation detections are not made when the calculations are repeated using shorter signal segments, fewer sensors or more distant stations. We demonstrate in addition how these almost repeating seismic sources have been exploited to detect and measure timing anomalies at individual sites within the arrays and network.

*Key words:* Cross-correlation, detection, seismic arrays, aftershocks

## 1 Introduction

Waveform correlation provides a method of detecting low-magnitude seismic events occurring in the close vicinity of sites at which previous events have generated high-quality, representative waveforms (Gibbons and Ringdal, 2006, and references therein). Correlation or matched filter detectors combine high sensitivity with a low false alarm rate since waveforms recorded at a given station are specific to a very limited source region (see, for example, Geller and Mueller, 1980). This property however also leads to the correlation detector's greatest drawback; it can only be applied in situations in which the form of the anticipated waveform is essentially known a priori, and it is still an open question as to how many monitoring situations exist where correlation detectors can reduce significantly the detection threshold for low magnitude seismic events. The proportion of events which are "repeating sources" is proving to be surprisingly high, in at least some regions (Schaff and Waldhauser, 2005; Schaff and Richards, 2004a,b). Whilst providing optimism for the applicability of a class of detectors that is entirely reliant upon waveform similarity between events, a number of questions require further investigation. For example, how far from a master event can a subsequent event be such that it can still be detected using waveforms from the master event as a template? Also, to what degree can the source mechanism and magnitude of two events vary whilst still resulting in a correlation detection? The answers to these questions are likely to be strongly dependent upon the geology at the source and on the path (see, for example, Nakahara, 2004) and the performance of correlation detectors is likely to vary greatly from region to region.

The International Monitoring System (IMS) of the Comprehensive nuclear-test-ban Treaty Organisation (CTBTO) is a sparse worldwide network of

*Email address:* steven@norsar.no (Steven J. Gibbons).

sensors installed in order to detect possible clandestine underground nuclear explosions which would constitute a violation of such a treaty. Seismic stations constitute a large component of the IMS and, given the demonstrable improvement in signal detectability which correlation detectors can provide over standard energy detectors, it is highly desirable to supplement the existing detection algorithms with sensitive and robust fully-automatic real-time correlation detectors in order to identify the occurrence of recognised signals wherever possible. In many circumstances, the motivation will be to ascribe with a high degree of confidence a detected signal to a known industrial source (see, for example Harris, 1991; Rivière-Barbier and Grant, 1993) such that analyst resources are not wasted upon identifying signals from uninteresting sources. Using waveform similarity to identify automatically aftershocks from major earthquakes is also desirable since the location of multiple events in long aftershock sequences can be very time-consuming and can lead to long delays in the production of comprehensive seismic bulletins. However, the primary motivation of this paper is to investigate the detectability (using matched filter detectors) of events which are too weak to be detected using conventional energy detectors at the distances imposed by the limitations of a sparse international network.

Many IMS seismic stations are arrays and Gibbons and Ringdal (2006) demonstrate how applying waveform correlation at multiple sites lowers the detection threshold significantly. Continuous correlation coefficient traces for different sites in a seismic array or network can be beamformed to give a single correlation function providing a significant array-gain. Unlike in traditional beamforming, where the channels are delayed according to the anticipated arrival time of a given phase, correlation coefficient traces are delayed simply according to the definition of the waveform templates. If the signal templates for different sites of a multi-channel matched filter detector all begin simultaneously, a zero-delay beam is applied regardless of the direction from which the signals arrive. Significantly, correlation coefficient traces are coherent over large aperture arrays and networks even when the actual waveforms are not. In the current paper, we will focus on the NORSAR array in Southern Norway (designated PS27 of the IMS). The large inter-site distances in this array, originally designed for the detection of weak teleseismic signals (Bungum et al., 1971), make the processing of regional phases by conventional means notoriously difficult due to the lack of waveform coherence across the array. Since waveform coherence is not a requirement for array-processing of correlation coefficient traces, the techniques presented here are readily applied to the NORSAR array and the results apply equally to seismic networks.

In addition to using waveform correlation for the purposes of signal detection, we exploit waveform similarity at both local and regional distances to provide the best possible constraints on the location of events. Waveform similarity alone was demonstrated by Menke (2001) to constrain the location of seismic

events using a simple model by which the correlation coefficient between the signals from two events decreased exponentially with event separation. More recently, Massa et al. (2006) have devised a fully-automatic quasi-real-time algorithm for locating events by cross-correlation using only a single seismic station. Shearer (1997), among others, demonstrates how events location estimates can be improved dramatically by the combined use of absolute arrival time readings with higher accuracy cross-correlation relative time measurements. The double difference procedures (see Waldhauser and Ellsworth, 2000; Waldhauser, 2001) apply such measurements taken over potentially enormous data sets to invert for multiple hypocenter estimates simultaneously.

A sequence of earthquakes in the Rana region of Northern Norway during 2005 has provided an excellent opportunity to study the extent to which small seismic events can be detected by signal matching at a distant station as a function of event magnitude and distance from a master event. Figure 1 shows the location of the largest event in the sequence in relation to the stations of the Norwegian National Seismic Network (NNSN), operated by the University of Bergen, and also to the Fennoscandian IMS seismic arrays NORSAR (PS27), ARCES (PS28), Hagfors (AS101) and FINES (PS17). The NNSN exists primarily for the investigation of earthquakes within Norwegian territory whereas the arrays were primarily installed to detect the signals from distant underground nuclear tests. Regional events are located automatically by the network of arrays by a judicious association of detected phases (Ringdal and Kværna, 1989) and Kennett (2002) illustrates how a seismic event very close to the sequence studied here is located to an acceptable accuracy by the network of arrays despite the absence of any very nearby stations. The earthquake sequence is particularly interesting for our purposes since the largest of the events (approximate magnitude 3.5) was well recorded by stations at quite large distances from the source, whereas many of the smaller events were not detected at the array stations by traditional energy detectors. The stations of the NNSN confirm the presence and timing of the smaller events and allow far better constraints to be applied to the locations of these earthquakes than would otherwise be possible.

Section 2 presents an overview of the events in the Rana region during 2005 which were observed at NORSAR and the other IMS arrays at distances exceeding 600 km. Given the observed waveform similarity of some of these events, we describe the development of a matched filter detector aimed at detecting occurrences of weaker events in this region. We discuss the limited number of detections obtained during 2005 using the large aperture NORSAR array and address how the validity of some of these can be supported by repeating the procedure on different array stations and thus providing independent observations.

Section 3 provides an overview of the closest stations of the NNSN to the

target region and demonstrate the improvement in location estimates which can be achieved using recordings from the closest stations. We display all the waveforms available which correspond to the times of the matched filter detections at NORSAR and conclude that almost all of the NORSAR detections correspond to real events in the Rana region.

Section 4 addresses the extent to which we are able to constrain the location of the detected events using recordings from local and from regional distances.

Finally, in Section 5, we summarize the detection and measurement of systematic timing errors on single sensors of the arrays using inconsistencies in the measurements of times of maximum cross-correlation.

## 2 A sequence of earthquakes in Northern Norway: Detections at the Nordic IMS array stations

The Rana region in Northern Norway is known for its relatively high constant seismicity (see, for example, Hicks et al., 2000) and is also the site of one of the largest known earthquakes in Fennoscandia in recent history ($M_s 5.8 - 6.2$ on August 31, 1819). Many regions on the north Norwegian coastline have been the sites of earthquake swarms; for example, Meløy between 1978 and 1979 (Bungum et al., 1979) and Steigen in 1992 (Atakan et al., 1994). Five events in this region during 2005 were large enough to be detected by more than one of the IMS array stations displayed in Figure 1; these are listed in Table 1. A few more events were detected by the ARCES array alone but, with estimated magnitudes well below 2.0, they were not included in the reviewed event bulletin. Waveforms from these events recorded at the NORSAR array are displayed in Figure 2. Since the events are almost due North of the array, the *be* and *bn* components of the broadband seismograms correspond almost to the transverse and radial rotations respectively; the *Sn* arrival is very much clearer on the horizontal components than the vertical components.

Figure 2 indicates that the signals recorded at NORSAR from these events have a good signal to noise ratio (SNR) in the frequency bands examined for at least three minutes following the initial P-arrival. To quantify the degree of waveform similarity for each pair of events, we calculate a fully-normalised correlation coefficient by sliding a waveform template from the first event over a selected time-window for the second event and recording the maximum correlation coefficient obtained. We in fact calculate an "array correlation coefficient" trace (c.f. Gibbons and Ringdal, 2006) which is a beam whereby the normalised correlation coefficient traces for the individual sites are delayed and averaged according to a set of imposed time-delays. Due to the large inter-site distances on the NORSAR array, the definition of the data-windows in

the waveform template is not trivial. For the definition of these templates, we define for each event a reference time $t_{\mathrm{R}}$ which, for simplicity, is an estimate of the event's origin time. For a fixed estimate of the event origin location (latitude, longitude and depth), we define the start of the time window for site $i$ as $t_{\mathrm{R}} + \tau_i$ where $\tau_i$ is the travel time of a specified seismic phase between source and receiver for the most appropriate one-dimensional velocity model (in this case, the Fennoscandian model, Mykkeltveit and Ringdal, 1981). For these templates, the master waveform for each site consists of 180.0 seconds of data beginning at the predicted *Pn*-arrival for the given master event. Whilst the time-windows for each channel ($\tau_i$) are in this case complicated functions of the master event origin location and chosen velocity model, provided that the same time-delays are applied by the detector as were used in the template definition, all subsequent correlation detection times, $t_{\mathrm{D}}$, are related only to the reference time, $t_{\mathrm{R}}$. A slightly different set of $\tau_i$ (for example, corresponding to a different location estimate or a different velocity model) will result in a different correlation coefficient but, providing that the templates contain largely the same data, the maximum correlation coefficient should occur at the same time and hence result in the same detection time, $t_{\mathrm{D}}$. If the time of the maximum correlation coefficient is not stable to small changes in the signal template specification, it is a sure indication that the observed waveform similarity is spurious or insignificant.

For each pair of events from the selected five, an array correlation coefficient was calculated in two different frequency bands; these are listed in Table 2. Three of the events considered (the events of April 28, June 24 and December 15) indicate a very high degree of waveform similarity with correlation coefficients exceeding 0.4 in both frequency bands for all event pairs. The events of May 1, 2005, and October 13, 2005, did not display a significant degree of waveform similarity with any of the other events with maximum correlation coefficients typical of those obtained between randomly selected data segments of the same length and bandpass filtering. For the given event pairs, the cross-correlation coefficient obtained in the 2.0-5.0 Hz frequency band is always greater than that obtained in the 3.0-8.0 Hz frequency band (i.e. the coefficients above the diagonal in Table 2 are greater than the corresponding values reflected in the diagonal). Although the SNR is greater at the higher frequencies, the wavelengths involved are shorter and the waveforms are hence more susceptible to distance between hypocenters and consequently smaller scale path heterogeneities. The events in Table 1 displaying the greatest degree of waveform similarity are the events on April 28 and June 24; despite over an order of magnitude difference in waveform amplitudes, the correlation coefficient exceeds 0.7 even for a three minute long data segment filtered between 3.0 and 8.0 Hz. The correlation coefficients obtained between the largest event (June 24) and the smaller events (April 28 and December 15) are greater than the correlation coefficient obtained between the two smaller events. This may be indicative of the relative locations of the three events or the result of the

larger magnitude of the June 24 event; waveform data from closer stations would be needed to address this.

A waveform correlation detector as described by Gibbons and Ringdal (2006) was prepared using the waveforms from the June 24 event as a signal template with the purpose of detecting seismic disturbances in the immediate vicinity of these earthquakes, too small to be detected by the IMS arrays using traditional energy detectors. Such disturbances could be either aftershocks immediately related to the largest events or nearby tremors at other times. It is clear from examining the correlation coefficients in Table 2 that each of the events April 28, June 24 and December 15 would be detected by such a system given the ratio between the maximum correlation coefficient obtained and the background values. A waveform template was defined as above, related to predicted *Pn*-arrivals at each site, but this time using a data segment of length 120.0 seconds, bandpass filtered between 2.0 and 8.0 Hz. The detector was run on continuous data from the NORSAR array for the whole of the calender year 2005. A detection threshold of 0.03 for the array correlation coefficient beam was exceeded a total of 32 times during this period; these instances are listed in Table 3.

The first task required is to check which of the correlation detections listed in Table 3 correspond to verifiable events in the Rana region. Detections 7, 23 and 30 clearly correspond to the April 28, June 24 and December 15 events in Table 1. Other detections have far more marginal correlation coefficients and may correspond to coincidental similarity with segments of noise or signals incident from other source regions. In addition to the low values of the correlation coefficients, the corresponding scaling factors (denoted $\alpha$ in Gibbons and Ringdal, 2006) are also very low for all the remaining detections. To make these numbers more tangible, we assign a magnitude 3.5 to the master event and estimate crudely that a scaling factor of $\alpha$ will correspond to a magnitude $M = \log_{10}(\alpha) + 3.5$. The magnitude estimates of 2.16 and 2.73 for the April 28 and December 15 events are slightly lower than (albeit of the same order as) the respective GBF magnitude estimates of 2.51 and 3.03.

A first approach to verifying the presence of events for each of these detections is to apply a similar procedure for each of the other IMS arrays displayed in Figure 1. Assuming that two events are co-located, and produce similar waveforms, then the time separating the corresponding patterns in the wavetrains will be identical for all stations (this is exactly the principle on which the beamforming of the correlation coefficient channels works). Therefore, assuming also that the SNR is sufficient for a detection, all stations should indicate an identical detection time (relative to the reference time for the master event). An analogous correlation detector was run over short time-windows surrounding each of the NORSAR detections in Table 3 for each of the remaining Nordic IMS array stations (ARCES, FINES, Hagfors and SPITS). Unlike the

detection procedure carried out using the NORSAR array, which correlated the waveform template against every possible data segment recorded during the year 2005, the detectors on the regional arrays have not yet been run continuously. A detection was made if and only if the maximum correlation coefficient attained exceeded the standard deviation for the whole time interval by a factor of 5 or more.

Table 4 displays the corresponding detection times for each of the arrays indicated for all of the 32 detections made on the NORSAR array. Despite the table offering no information other than a time of maximum correlation (or an indication that no detection was made), many remarkable observations are possible. The first is that the essentially equidistant ARCES array (25 sites within an aperture of approximately 3 km) reports a detection within a small fraction of second for every one but two of the correlation detections made by the NORSAR array. The first of these detections (on January 25) was not detected by any of the other array stations and the arrival of a strong teleseismic P-phase within the two minutes following this time indicates a high probability that this marginal correlation is a false alarm. Nothing further can be inferred about an event on 6 April 2005 since ARCES suffered a power outage at this time and any event, if present, was too weak to be detected by any of the more distant arrays. Given that these 32 detections are the only occasions on which this matched filter detector triggered within the space of a calender year, and that 30 of these are matched to within no more than 0.15 seconds by entirely independent array observations from almost the opposite backazimuth indicates that the likelihood that this detection list contains a large number of false alarms is very small.

The second major observation from Table 4 is the small amount by which the detection reference times differ. Almost all the values quoted are zero to within at most a few samples (the NORSAR, ARCES and FINES arrays are sampled at 40 Hz whilst SPITS and HFS are sampled at 80 Hz). For a sampling interval of 0.025 seconds, the 5 decimal places quoted in Table 4 appear excessive given that this precision is the combination of both FIR-filter resampling of the waveforms and a spline interpolation of the correlation coefficient traces. However, an accuracy of 0.001 seconds is quite reasonable for such cross-correlation calculations (see, for example, Poupinet et al., 1984) which means that the additional decimal places are required simply to eliminate the effect of numerical round-off in arithmetic. Three factors contribute to a non-zero difference between detection times at different stations:

(1) a distance between the hypocenters of two subsequent seismic events will lead to changes in the relative travel times to different receiver sites.
(2) waveform dissimilarity (be it the result of differences in the source, the path, or background noise in the case of a low signal-to-noise ratio at the receiver) will lead to correlation coefficient traces which may not result

in a maximum value at the expected time.
(3) systematic timing problems at the receiver.

Aside from single site aberrations, which are discussed further in Section 5, only one systematic timing error is known to exist in the array data used in this paper. The Spitsbergen array, between August 3 2005 and December 31 2005, put a time stamp on data which was one second ahead of Universal Time; this was the result of a manufacturing error, announced and documented by the supplier of the instruments, to compensate for the leap second on December 31, 2005. If data from this array had not been duly corrected prior to the analysis, the entry for SPI for detection 30 would read $-1.0390$.

The non-zero entries in Table 4 are therefore presumably due to a combination of the first two factors stated above. There are very few values which are clearly anomalous, $\delta t$ at HFS for detection 9 being an obvious exception. The Hagfors array in fact shows the smallest deviations from the detection times at the NORSAR array; being the array which is geographically closest to the NORSAR array, the small $\delta t$ at HFS suggest that the $\delta t$ are dominated by varying locations of the events. The close correspondance between the maximum correlation times at the full ARCES array and the nine element subset (denoted rARC) suggests that waveform dissimilarity does not contribute greatly to the changes in time measurements; were waveform dissimilarity significant, the additional correlation coefficient channels added when the whole array is considered would probably have a far greater effect on the estimated time of maximum correlation. The $\delta t$ for the regional arrays relative to NORSAR in the first half of the year appear to be largely positive and those towards the latter part of the year appear to be largely negative. This could indicate a systematic shift (for example drift along a fault) of hypocenter locations, although we would be required to take separate measurements for P- and S- phases and demonstrate their consistency in order to be able explain the differences.

A further piece of information provided by Table 4 relates to the detectability of the various events by the different arrays. Since the full and continuous detection process was only run on the NORSAR array, we assume that the 32 detections shown are the only ones obtainable in this period. (It is of course possible that a continuous detector run on the ARCES array would detect further events not picked up by NORSAR.) As previously stated, the full ARCES array resulted in detections which matched all but two of the NORSAR detections. The reduced ARCES array fails to pick up a further four of these detections. The reduced configuration, consisting of the central element and the eigth instruments contained in the innermost A and B rings, was purposefully chosen since this design most closely matches the standard by which most new array installations are being designed. It also provides a closer comparison with the Hagfors array, which shows a similar detection

capability although does make slightly fewer detections; this could be partly due to the slightly greater distance from the source. It could also be the result of different noise conditions at the arrays or differences in signal attenuation along the propagation paths.

The FINES array is at a slightly greater distance again than the Hagfors array and, whilst consisting of 16 sites as opposed to the nine at Hagfors, matches significantly fewer of the NORSAR detections. Nevertheless, 14 out of a possible 32 detections are matched and each with a very small time-residual. The nine-site Spitsbergen array at a distance of over 1300 km is only able to detect the two largest events of April 28 and December 15 using the signal from the June 24 event as a master waveform template. Whilst not assisting our search for further events from this region, this is an encouraging result in the field of CTBT monitoring since the signal resulting from this magnitude 3.5 event registered a fairly low SNR at the SPITS array and yet using a matched field detector with this weak signal is nevertheless able to detect two events of up to an order of magnitude smaller.

The final comment to be made about Tables 3 and 4 is that several of the detections occur in quick succession of each other. In the cases of the detections on, for example, June 10 and June 24 there is approximately an hour separating each of the correlation detections. Assuming that each of these detections does actually correspond to a real event, the fact that each of the detections is distinct (i.e. the time separating the detections is far longer than the length of the waveform template) means that each must correspond to a distinct event. The sequences of detections on April 28 and December 15 are more difficult to judge without additional information; only 42 seconds separate detections 30 and 31 (on December 15) and so the second detection comes during the wavetrain corresponding to the first detection. One indication that the detections correspond to distinct events, rather than that the coda from these events show a great degree of self-similarity after a certain number of seconds, is the fact that the ARCES and Hagfors arrays both give independent confirmation of these detection times. Given the great dissimilarity of the waveforms registered at the different arrays, it would be highly unlikely that such a repeating waveform pattern would recur at exactly the same time interval and, besides, one would have expected the same behaviour for each of the main events which is not the case.

Figure 3 shows the sequence of detections occurring on December 15, 2005. We demonstrate here that the weakest of these detections (detection 31 in Table 3) is not possible when a data segment of only one minute, beginning at the *Pn* arrival, is used. Assuming that this secondary detection does indeed correspond to a small aftershock, the timing is such that a minute of P-coda from the aftershock arrives at the NORSAR array at the same time as the greatest amplitudes in the regional wavetrain: the *Sn* and *Lg* phases. A possible

corollary is that, when selecting data segments for correlation detectors, it is more important to select a section of the signal with the largest amplitude than a segment containing the start of the wavetrain.

## 3 Observations of events from stations of the Norwegian National Seismic Network (NNSN)

Figure 4 indicates the locations of the five NNSN stations which are closest to the Rana sequence, together with two location estimates for the June 24 main event. The white circle indicates the location estimate obtained using only the Fennoscandian IMS arrays. The location estimate indicated by the star (66.409°N, 13.324°E with depth 13.33km) was obtained using the HYPOSAT program (Schweitzer, 2001a) using only P- and S- picks, together with polarisation based P-phase azimuth and slowness estimates, from the waveforms displayed. The Stokkvågen station, STOK, is situated to the South-West of this sequence and has been a part of the NNSN since the summer of 2003. Figure 4 shows how the S-arrival at STOK is over an order of magnitude larger than the P-arrival on all components. This is not the case for the temporary STOK1 station to the North-West of the events; here, the P-amplitude is of the same order as S- on the vertical and radial components.

Unlike the IMS array stations, which record and archive continuous data, most of the NNSN stations are triggered and it is often not possible to inspect data for a requested time-interval in the past. However, as displayed in Figure 5, the STOK station did archive data for the time-intervals corresponding to almost all of the 32 correlation detections at NORSAR. With the waveforms aligned according to greatest correlation coefficient for a window following the S-arrival, these signals appear almost identical at a glance; they are only differentiated by the large differences in amplitudes. Over three orders of magnitude separate the amplitudes for detections 21 and 23 which, given the waveform similarity, allows us to conclude an approximate three orders of magnitude difference in the corresponding event magnitudes. For the P-arrivals to be compared meaningfully, they are displayed in a magnified window in the left panel of Figure 5. It is clear that the events cannot be precisely co-located since there is a measurable difference in the S-P travel times. Figure 5 also resolves the issue of the aftershock sequences on April 28 and December 15, confirming that the detections on the NORSAR array (see Figure 3) do in fact correspond to distinct events. The weak P-arrival at STOK for detection 31 fails to exceed the coda of the much larger event which occurred 45 seconds previously. The other detection for which no P-arrival is visible in Figure 5 is number 9; this is clearly two events occurring a rapid succession of each other and the arrival in the left panel is actually the S-phase from the previous event.

It should be noted that, for the detections prior to June 2005, the absolute time at the STOK station cannot be relied upon due to a technical problem with the GPS receiver. The fault was repaired and detections including and following June 10, 2005, are recorded with a correct absolute time. By comparing the time elapsed between events at the IMS arrays and at the STOK station prior to June 2005, we can confirm that the drift never exceeded 0.3 seconds. However, since this value is very much larger than the uncertainty in the phase picks at the station, only differential S-P times can be used from STOK during this period. It is clear that, for the events displayed in Figure 5, the S-P time difference is identical to within approximately 0.05 seconds. Based upon a P-velocity of 6.20kms$^{-1}$ and a $v_{\mathrm{P}} : v_{\mathrm{S}}$ ratio of 1.73, this would mean that the hypocentral distance to the STOK station is the same for all events to within approximately 450 m.

The temporary station STOK1 was deployed in June 2005 to the North-West of the cluster and, based upon S-P traveltime differences, is probably marginally closer than STOK. Due to technical and logistical difficulties, this station unfortunately recorded only 8 of the detected events; the waveforms are displayed in Figure 6, again aligned according to maximum waveform similarity for the S-arrival. The signals on the horizontal components are very similar for each of the events shown, whereas the vertical component recordings appear to show a progressive change. For this limited number of events, an inspection of the P-arrivals (with alignment according to the S-wave cross-correlation) suggests an even lower range of hypocentral separations in the direction of the STOK1 station than was shown for the STOK station.

Given the similarity of the different signals on the horizontal components of the STOK1 station, we can again infer that the amplitude ratios give a reasonable indication of the event magnitudes. Both STOK and STOK1 recorded the main June 24 event and, if we fix the estimated magnitude of this event (we have used 3.5 consistently within this paper), we may calculate magnitude estimates for the other events, $i$, using

$$m_i^S = \log_{10}(\alpha_i^S) + 3.5 \tag{1}$$

where $\alpha_i^S$ is the ratio for station $S$ between the maximum amplitude of the S-wave for event $i$ and the maximum S-wave amplitude for the master event. If this formulation is valid, then the $m_i^S$ should be essentially independent of the station, $S$. This is confirmed for the limited number of events recorded by both STOK and STOK1 in Figure 7 where the filled symbols indicate a close correspondence. The amplitude ratios measured at the local stations indicate the smallest of the events detected by the matched filter on the distant NORSAR array were of magnitudes as low as 0.5.

The open symbols in Figure 7 indicate the relationship between the magnitude

estimates obtained from the NORSAR correlation calculations and the magnitude estimates obtained from the STOK recordings. The correspondence is surprisingly good considering the low SNR of the signals at the distant array station, although there is a tendency for the array inversions to underestimate the magnitude, especially for the smaller events. The scaling factors, $\alpha$, inverted from the correlation calculation (described in detail by Gibbons and Ringdal, 2006), are too low by up to half a magnitude unit with the disparity increasing as the SNR decreases. The inversion does appear to provide a useful lower bound on the magnitude estimate.

An additional temporary station, STOK2, was also deployed later in the summer of 2005; based upon S-P travel time differences, this station appears to be the closest of the three. Unfortunately, this is also the station for which we have the fewest recordings with only four of the events in this sequence recorded (see Figure 8). This is not only unfortunate from the perspective of locating the events, but because the waveforms at this station show the greatest variation from event to event. The September 12 and September 24 events in Figure 8 resulted in almost identical waveforms, whereas all other event pairs display significant differences, both in the alignment of features and in the relative size of the P- and S- arrivals. For the STOK and STOK1 stations, the part of the wavetrain which displayed the greatest similarity from event to event was the S-arrival. For the STOK2 station, it is the P-arrival and so the waveforms displayed in Figure 8 are aligned according to the maximum correlation coefficient at the time of the P-arrival.

Finally, it should be noted that for the detections which were not recorded by the Stokkvågen stations, only detection number 1 in Table 3 was not supported by observations from any of the NNSN stations.

## 4 The location of events detected

Under ideal circumstances, we would have a complete record of every event in the sequence from the local network with which we could calculate accurate relative delay times and solve for the locations of the entire sequence simultaneously using the double-difference algorithm as implemented in the hypoDD program (Waldhauser and Ellsworth, 2000; Waldhauser, 2001). As we can see from Figures 5, 6 and 8, the set of recordings at nearby stations is far from complete, the shortfall of data being compounded by a timing error for the STOK station prior to June 10, 2005. Only a single event in this sequence is in fact recorded by all three stations STOK, STOK1, and STOK2; this is the magnitude 0.8 event on October 19, 2005.

Figure 9 indicates the limitations which the available set of recordings places

upon the location algorithms which we have attempted to apply to this set of events. Panel (a) indicates locations obtained using HYPOSAT with all satisfactory arrival time picks and polarisation angles from the local network. Whilst the greatest number of events fall within the region indicated in Figure 4, the spread is large and the events located at the greatest distance from the best estimate so far of the June 24 event (66.409°N, 13.324°E with depth 13.33km) are demonstrably those with the poorest data coverage. The worst case events had only P- and S- arrival estimates, together with a polarisation angle for the P-arrival from a single station: in other words, the absolute minimum requirement for any form of location estimate. This is clearly a very unsatisfactory basis for a comparison of location estimates but is also typical for what a sparse network might have available for events of such low magnitude.

As is displayed in Figures, 5, 6 and 8, there is a great deal of waveform similarity between events and high-accuracy cross-correlation delay times were calculated for both P- and S- arrivals for these three stations. In only a very few cases was the correlation coefficient so poor that a clear time differential was not observable. P-arrivals at MOR8 were also very similar from event to event and were used to calculate delay times; very little similarity was observed for S-arrivals at MOR8. In principle, the hypoDD program (Waldhauser, 2001) can apply such a combination of absolute picks and differential times in a simultaneous hypocenter inversion; it is, however, unclear a priori as to whether the data coverage for this set of events is suffcient. Panel b) of Figure 9 shows a hypoDD relocation where the initial conditions are provided by the HYPOSAT solutions displayed in panel a). Note that many of the hypocenters are now far more concentrated but that there is an almost linear spread of the remaining events. We note that almost all of the outlier events are those prior to June for which STOK recordings were not used due to the demonstrable timing problem. Since these events also preceded the deployment of the STOK1 and STOK2 instruments, they are constrained almost entirely by the MOR8 and NSS stations. The linearity of these locations thus almost certainly reflects the station coverage rather than any geophysical features.

We can demonstrate further that the outlier location estimates in Figure 9 b) are not stable to changes in the location procedure. hypoDD can use a single source starting location and the results for this inversion are shown in panel c) of Figure 9 with the initial location given in the figure caption. Many events are deleted during the inversion process if, at any iteration, they become located above the free surface (see Waldhauser, 2001). The outlier observed to the North-West is the main April 28 event where the horizontal displacement is compensated for in the solution by a shallower depth. A final test for the location stability of this data set using hypoDD is demonstrated in panel d) where the initial location used was a zero depth at the same surface location

as used in panel c). The events which are not removed during the inversion are placed close to the surface slightly to the North-East of the assumed location of the cluster.

Whilst we would ideally eliminate the effects of station coverage by reducing to a "lowest common denominator" set of observations, the simple fact is that in doing so only a very limited set of events could be considered simultaneously. Whilst we are unable to state categorically that all of these events occurred within a region of a given size, we have been unable to provide a robust demonstration that any two events must be separated by a significant distance.

## 5 The use of closely located seismic events for the identification and correction of systematic timing errors

Gibbons and Ringdal (2006) alluded to the idea that the synchronicity of the correlation maxima should be examined, not only to check the validity of the correlation detection but also to expose any timing discrepancies between stations. Exactly such a situation arose during the current study whereby two channels of the NORSAR array developed a timing disparity in the summer of 2005 due to a defective GPS receiver. Panel (a) of Figure 10 shows the correlation peaks on selected channels of the NORSAR array (together with the beam from all 42 sites) from the correlation of the main shocks on June 24 and April 28, 2005. The master waveform template included both primary and secondary phases and was band-pass filtered in a wide frequency band; any differences in the times of maximum correlation at the different array sites resulting from small changes in the source to receiver paths are too small to be measurable from this calculation. The elements NAO05 and NC601 produce a maximum correlation coefficient at times which are not consistent with the remaining array elements. The multi-channel cross-correlation and least squares method of VanDecar and Crosson (1990) is ideal for making accurate measurements of the time-delays involved; to the nearest 0.001 seconds, NC601 and NAO05 attain respectively a correlation maximum 0.538 seconds after and 1.723 seconds before the common correlation time.

The limitations of this method of time synchronisation verification are clear; we require two events that have produced high SNR signals to have occurred sufficiently close to eachother that waveform comparison produces a single signficant maximum correlation peak. For a given array or network, it may be many weeks, months or years between the occurrence (if ever) of such fortuitous seismic events. Most other methods exploit waveform similarity between sensors, either for strong phase arrivals or for microseismic noise (see Koch and Stammler, 2003, and references therein); the exploitation of background noise is particularly helpful since it is not dependent upon the occurrence of

satisfactory seismic events. However, the quality control illustrated in Figure 10 is valid for an arbitrary configuration of stations (provided that all stations record both events sufficiently well) and requires neither coherence of a wavefront over a network or knowledge of the wavefield from a given source. Panel (b) of Figure 10 illustrates the difficulty of measuring time discrepancies based upon even a strong teleseismic arrival. Whilst the elements NC601 and NAO05 are clearly anomalous, we can only deduce the timing discrepancy indirectly by measuring the relative delay times for each pair of channels and then judging which delays ought to be observed for the given incoming wavefront. The measurement of the relative delay times (c.f. VanDecar and Crosson, 1990) is far more problematic with real seismic signals than with the symmetric correlation coefficient traces. Whereas the time of the peak of the correlation traces is largely independent of the frequency band applied, the signal coherency decreases dramatically with increasing frequency and relative time-delay measurements can vary greatly depending upon the choice of time-window. The plane wavefront models fail notoriously for the NORSAR array (see, for example, Berteussen, 1976) with little concensus as to what degree the observed anomalies are the result of local effects or distant heterogeneities (e.g. Pritchard et al., 2000). The locations of the markers relative to the features on the waveforms in panel (b) of Figure 10 illustrate the shortcomings of the best-fit plane-wave model.

An additional problem can be observed for the SPB3 instrument of the Spitsbergen array in Figure 10 (c), which is also the result of a defective GPS receiver. The correlation between these two very low SNR signals is more than sufficient to identify the problem but too poor to be able to calculate a high-precision estimate for the timing anomaly.

A comparison between the differential reference times obtained by correlation at the array stations (Table 4) and the differential times obtained at the STOK station confirm the known drift (to within approximately 0.3 seconds) which occurred at this station as the result of a GPS receiver problem prior to June 2005. Unfortunately, without additional instruments closeby, we are not able to measure directly this drift using these reference events. The calculation of the timing discrepancy on the NORSAR array was possible since the delays on all but two of the 42 sites were measured to zero to the limit of the accuracy permitted by the available waveforms. (This is to say that differences in event-to-event travel time differentials between sites on the array are not detectable.) For the short distances involved for the local network, this is not the case and we have demonstrated clear differences in in S-P times from event to event at the closest stations. However, in a multi-event hypocenter location solution, where the S-P times from the STOK station are given high weights and the absolute time picks are given a high uncertainty value, a reasonable estimate of the drift at the time of each of the events located should be possible.

## 6 Conclusions

We have identified five seismic events exceeding magnitude 2.0 which occurred in the Rana region of northern Norway during the calender year 2005; these were the only such events from this region during this period to be detected by more than one IMS seismic station, all of which are at distances in excess of 600 km. Three of the events, including the largest (magnitude 3.5 on June 24, 2005), generated very similar signals at the IMS array stations; three minute long waveform segments at the large aperture NORSAR array resulted in very high correlation coefficients even when bandpass filtered between 3 and 8 Hz. In an attempt to find further seismic events of lower magnitude from the vicinity of the source of the largest event, an on-line correlation detector was initiated using the waveforms generated by this event, recorded at the NORSAR array, as a signal template. When run on continuous NORSAR data for the whole of 2005, a total of 32 clear detections were made. Almost all of these detections occurred at times when no signal detectable by traditional energy detectors was observed.

The validity of 30 of these correlation detections was confirmed beyond reasonable doubt by applying similar correlation detectors to the other Nordic IMS array stations; all but two of the matched filter detections at NORSAR occurred within a small fraction of a second of an independent, corresponding detection at at least one of the other arrays. 31 out of the 32 detections are confirmed to correspond to low magnitude events in the Rana region by closer stations of the Norwegian National Seismic Network (NNSN); the remaining detection at NORSAR is presumed to be a false alarm. Many of the correlation detections occurred during the coda of the largest events. The synchronicity of these subsequent detections at each of the different arrays indicated that these probably corresponded to distinct small aftershocks and this was duly confirmed by examining the data from the local stations.

Many of these coda events were missed if too short a waveform template was used; the signal template should include the part of the wavetrain containing the greatest amplitudes. When using conventional energy detectors, the start of the signal is the most important since this is where the highest SNR is observed (STA/LTA detectors are optimal for impulsive signals). Correlation detectors work by the recognition of waveforms and are unaffected by the SNR in the STA/LTA sense; only the ratio of the signal amplitude to the background noise is important. They are consequently as effective with emergent signals as with impulsive signals and there may be many cases whereby the optimal template for detecting an event at a given station does not include the initial arrivals.

Although the recordings of the sequence by the local network are very incom-

plete, the signals that exist are of a very high quality and indicate that events detected clearly by the distant NORSAR array are of magnitudes as low as 0.5. This is significant for two reasons. Firstly, this represents at least an order of magnitude improvement in the detection capability for the network of arrays. (In practice, the effective improvement in detection capability is even greater since even events of magnitudes 2.0 at this distance are only detected with confidence by the ARCES array and may thus be associated with a large location error.) Secondly, the events were detected using a signal template from an event three orders of magnitude larger.

Whilst the incompleteness of the local network recordings precludes a comprehensive double-difference location of the full set of events, the measurable differential travel times from the local stations at three very different azimuths from the presumed hypocenter locations do suggest that the event locations cannot be separated by more than approximately 0.5km in any direction.

We have demonstrated additionally that events which are as closely located as those in this sequence can be exploited to expose systematic timing anomalies which effect one or more sites within an array or network. When such repeating seismic events occur, highly accurate measurements of the timing discrepancy can be made without the need to calibrate for the observed arrival pattern of the incoming wavefront.

## 7 Discussion and Recommendations

We purposefully restricted the current study to seismicity in this very limited region occurring during the calender year 2005. The whole region has demonstrated regular seismic activity for as long as it has been observed (see, for example, Hicks et al., 2000, and references therein) and there is a high possibility that many more occurrences of similar events from this region would be identified by continuing the detection process both backwards and forwards in time. The waveform correlation detector described in this paper is now run continuously on all incoming NORSAR data and, already within the first three months of 2006, three almost co-located events were detected and confirmed by stations of the NNSN (origin times of 2006-056:23.14.49.050, 2006-068:20.52.58.800 and 2006-085:08.03.53.425). The seismicity in the greater Rana region has been demonstrated by Hicks et al. (2000) to occur in many different geographical clusters and, based on the current work alone, it is impossible to tell whether the waveform similarity (and hence event detectability) observed here will be equally applicable to other regions of Nordland, let alone in the even wider global context.

In addition to the problem of geographical portability, there is the question of

how the performance of such detectors would vary with the recording network available. The situation in the current paper is as close to ideal for this task as is possible; there is no region on earth with a greater density of IMS array stations, backed up by a national network of seismometers to confirm the findings. The hypothesis of Gibbons and Ringdal (2006) that such methods, when applicable, ought to reduce the detection threshold by approximately an order of magnitude appears to hold still; the detection of the April 28 and December 15 events on the Spitsbergen array at over 1300 km is as important in the context of explosion monitoring as the detection of the numerous small tremors and aftershocks by the array stations at half that distance.

Also of great interest to the field of seismic monitoring is the ability to detect earthquake aftershocks even within the coda of events well in excess of an order of magnitude larger using only a single array station. Richards and Kim (1997) pointed out that a clear aftershock following the 16 August 1997, magnitude 3.5, Kara Sea event made it highly unlikely that the event had been a clandestine explosion as was originally hypothesised. If a correlation detector can resolve one or more clear aftershocks from the incoherent coda as was demonstrated in Figure 3, this could constitute a rapid and significant step in the source discrimination process.

Correlation detectors were employed at the regional Fennoscandian array stations over short time segments to verify the validity of detections made at the NORSAR array. However, a single preliminary attempt to perform the full continuous process at ARCES resulted in a huge number of detections, the majority of which clearly did not correspond to events in the Rana region. This phenomenon is characteristic of the regional seismic arrays (see Gibbons and Ringdal, 2006) and occurs simply because of the high coherence of the actual waveforms between sensors. Even when two waveforms which essentially bear little resemblance are correlated, the single channel correlation functions are likely to exhibit a similar behaviour within a short time-window, leading to a beam gain which would not be observed on a large aperture array or seismic network. In the case study examined by Gibbons and Ringdal (2006), almost all of these false alarms were eliminated by detecting a "non-zero apparent velocity" in the actual correlation coefficient traces. That elementary test is more difficult to apply when using long time windows as in the example here simply because the correlation maxima are unlikely to be dominated by the contribution from one single short time-window, and so degrading the validity of the plane-wave assumption which made the technique so successful in Gibbons and Ringdal (2006). The same principles will still be able to be applied but more care must be taken to identify exactly which parts of the time-series dominate the correlation coefficient, and use these shorter time windows for estimating the apparent velocity.

The accurate relocation of a small number of events using temporary stations

at local distances and cross-correlation differential traveltime measurements can facilitate a calibration for more distant stations which can lead to a dramatic improvement in the accuracy of subsequent location estimates by conventional means. Figure 4 shows the original location estimate for the June 24, 2005, event from Table 1 together with the relocation performed using the local network. The error ellipses associated with the locations of seismic events are likely to increase with decreasing event magnitude because the decreasing SNR of the signals will lead to greater errors in arrival time picks and slowness and azimuth measurements. However, the improved event locations for certain regions may allow correction for some of the systematic bias in the array-only estimates. The event is mislocated by approximately 20 km to the East, which is not very surprising given the azimuth coverage of the Fennoscandian array stations. The mislocation is consistent with the slowness estimate biases observed by Schweitzer (2001b); see also Kværna et al. (2005). In situations where events are only well observed by a single array station, the application of carefully calibrated traveltime and azimuth corrections may lead to a dramatic improvement in location estimates (Gibbons et al., 2005).

It is unlcear as to how long the STOK1 and STOK2 stations will remain in the field. It was originally intended that they be removed during the summer of 2006, but this decision may be overturned in the light of the excellent recordings which have been produced of small seismic events in various clusters in the Rana region. These stations, together with the permanent Stokkvågen station, STOK, have permitted a far greater event location accuracy than has been available previously. Many events both prior to and following the placement of the temporary network may now be better constrained by considering waveform similarity at regional distances with the accurately located events from this period. Financial limitations prevent the installation of stations close to every site with seismicity of interest. This work may be of interest to the monitoring of small earthquakes in remote regions where it is logistically difficult or prohibitively expensive to maintain a permanent local network.

We recommend that a large-scale effort be made to continue the identification of repeating seismic sources in line with the work of Schaff and Waldhauser (2005). This will serve the manifold purposes of increasing our knowledge of the distribution of seismicity, reducing the detection threshold for low-magnitude seismic events, obtaining more accurate location estimates, and providing large banks of test events with which continual quality control of instrumental timing can be carried out.

The availability of historical recordings from seismic stations is essential if the accumulating database of seismic recordings is to be best utilised for the detection and interpretation of subsequent seismic events. The large-aperture NORSAR array is demonstrably not well-suited to the detection and identification of weak regional seismic phases using conventional energy detectors,

which is the current emphasis in the field of nuclear explosion monitoring. It has been argued, therefore, that a spatial redesign of the array would make it a more useful IMS station. Given the now thirty-five year history of high-quality digital seismic data from NORSAR, containing one of the most comprehensive archives of nuclear explosion recordings in existence, the increasing importance of waveform correlation detectors offers the strongest possible argument against a relocation of sites within the array.

The improvement in event detectability with an increasing number of sensors in an array (irrespective of array geometry) is usually greater for correlation detectors than the corresponding improvement for energy detectors. This is because, for traditional array processing, additional sensors only improve the SNR significantly if the new channel reinforces the observed signal and simultaneously suppresses noise (see, for example, Kværna, 1989). For the correlation detectors, the condition of waveform coherence over the array is replaced with the condition of waveform similarity between the signal template and the incoming data stream (Gibbons and Ringdal, 2006) and this means that additional sensors at essentially arbitrary positions can (provided that the single-channel SNR is not significantly worse) only improve the array correlation beam. We have observed in this paper that a reduction in the number of array elements at a given distance does reduce the detectability using waveform correlation and we conclude that the newer 9-site regional arrays in the IMS will provide less effective correlation detectors than the older arrays with a greater number of sites and a larger aperture.

## Acknowledgements

This material is based upon work supported by the Department of Energy (National Nuclear Security Administration) under Award Number DE-FC52-05NA26604.

The Norwegian National Seismic Network is operated by the Department of Earth Science, University of Bergen, Norway and supported by Oljeindustriens Lands Forening (OLF) and the Faculty of Mathematics and Natural Sciences, University of Bergen.

We are grateful to Jens Havskov and Kuvvet Atakan for valuable discussions regarding seismicity in the Rana region.

Maps were created using GMT software (Wessel and Smith, 1995).

## Disclaimer



## References

Atakan, K., Lindholm, C. D., Havskov, J., 1994. Earthquake swarm in steigen, northern norway: an unusual example of intraplate seismicity. Terra Nova 6, 180–194.

Berteussen, K. A., 1976. The origin of slowness and azimuth anomalies at large arrays. Bull. Seism. Soc. Am. 66, 719–741.

Bungum, H., Hokland, B. K., Husebye, E. S., Ringdal, F., 1979. An exceptional intraplate earthquake sequence in meløy, northern norway. Nature 280, 32–35.

Bungum, H., Husebye, E. S., Ringdal, F., 1971. The NORSAR array and preliminary results of data analysis. Geophys. J. R. astr. Soc. 25, 115–126.

Geller, R. J., Mueller, C. S., 1980. Four Similar Earthquakes in Central California. Geophys. Res. Lett. 7 (10), 821–824.

Gibbons, S. J., Kværna, T., Ringdal, F., 2005. Monitoring of seismic events from a specific source region using a single regional array: a case study. J. Seismology 9, 277–294.

Gibbons, S. J., Ringdal, F., 2006. The detection of low magnitude seismic events using array-based waveform correlation. Geophys. J. Int. 165, 149–166, doi: 10.1111/j.1365-246X.2006.02865.x.

Harris, D. B., 1991. A waveform correlation method for identifying quarry explosions. Bull. seism. Soc. Am. 81, 2395–2418.

Hicks, E. C., Bungum, H., Lindholm, C. D., 2000. Seismic activity, inferred crustal stresses and seismotectonics in the rana region, northern norway. Quaternary Science Reviews 19, 1423–1436.

Kennett, B. L. N., 2002. The Seismic Wavefield. Volume II: Interpretation of Seismograms on Regional and Global Scales. Cambridge University Press.

Koch, K., Stammler, K., 2003. Detection and Elimination of Time Synchronization Problems for the GERESS Array by Correlating Microseismic Noise. Seism. Res. Lett. 74 (6), 803–816.

Kværna, T., 1989. On exploitation of small-aperture NORESS type arrays for enhanced p-wave detectability. Bull. seism. Soc. Am. 79, 888–900.

Kværna, T., Gibbons, S. J., Ringdal, F., Harris, D. B., 2005. Integrated Seismic Event Detection and Location by Advanced Array Processing. In: Proceedings of the 27th Seismic Research Review, Rancho Mirage, California, September 2005. Ground-based Nuclear Explosion Monitoring Technologies. pp. 927–936.

Massa, M., Ferretti, G., Spallarossa, D., Eva, C., 2006. Improving automatic location procedure by waveform similarity analysis: An application in the South Western Alps (Italy). Phys. Earth Planet. Inter. 154, 18–29.

Menke, W., 2001. Using Waveform Similarity to Constrain Earthquake Locations. Bull. seism. Soc. Am. 89 (4), 1143–1146.

Mykkeltveit, S., Ringdal, F., 1981. Phase identification and event location at regional distances using small-aperture array data. In: Husebye, E. S., Mykkeltveit, S. (Eds.), Identification of seismic sources - Earthquake or underground explosions. Reidel Publishing Company, pp. 467–481.

Nakahara, H., 2004. Correlation distance of waveforms for closely located events - I. Implications of the heterogeneous structure around the source region of the 1995 Hyogo-Ken Nanbu, Japan, earthquake ($M_W = 6.9$). Geophys. J. Int. 157, 1255–1268.

Poupinet, G., Ellsworth, W. L., Frechet, J., 1984. Monitoring Velocity Variations in the Crust Using Earthquake Doublets: An Application to the Calaveras Fault, California. J. Geophys. Res. 89, 5719–5731.

Pritchard, M. J., Foulger, G. R., Julian, B. R., Fyen, J., 2000. Constraints on a plume in the mid-mantle beneath the Iceland region from seismic array data. Geophys. J. Int. 143, 119–128.

Richards, P. G., Kim, W.-Y., 1997. Testing the nuclear test-ban treaty. Nature 389, 781–782.

Ringdal, F., Kværna, T., 1989. A multi-channel processing approach to real time network detection, phase association, and threshold monitoring. Bull. seism. Soc. Am. 79, 1927–1940.

Rivière-Barbier, F., Grant, L. T., 1993. Identification and Location of Closely Spaced Mining Events. Bull. seism. Soc. Am. 83, 1527–1546.

Schaff, D. P., Richards, P. G., 2004a. *Lg*-Wave Cross Correlation and Double-Difference Location: Application to the 1999 Xiuyan, China, Sequence. Bull. seism. Soc. Am. 94, 867–879.

Schaff, D. P., Richards, P. G., 2004b. Repeating Seismic Events in China. Science 303, 1176–1178.

Schaff, D. P., Waldhauser, F., 2005. Waveform Cross-Correlation-Based Differential Travel-Time Measurements at the Northern California Seismic Network. Bull. seism. Soc. Am. 95, 2446–2461.

Schweitzer, J., 2001a. HYPOSAT - an enhanced routine to locate seismic

events. Pure appl. geophys. 158, 277–289.
Schweitzer, J., 2001b. Slowness corrections - one way to improve idc products. Pure appl. geophys. 158, 375–396.
Shearer, P. M., 1997. Improving local earthquake locations using the L1 norm and waveform cross correlation: Application to the Whittier Narrows, California, aftershock sequence. J. Geophys. Res. 102, 8269–8283.
VanDecar, J. C., Crosson, R. S., 1990. Determination of Teleseismic Relative Phase Arrival Times Using Multi-Channel Cross-Correlation and Least Squares. Bull. seism. Soc. Am. 80, 150–169.
Waldhauser, F., 2001. hypoDD – A program to compute double-difference hypocenter locations. Tech. Rep. Open-File Report 01-113, U.S. Geological Survey.
Waldhauser, F., Ellsworth, W. L., 2000. A Double-Difference Earthquake Location Algorithm: Method and Application to the Northern Hayward Fault, California. Bull. Seism. Soc. Am. 90 (6), 1353–1368.
Wessel, P., Smith, W. H. F., 1995. New version of the Generic Mapping Tools. EOS Trans. Am. Geophys. Union 76, 329.

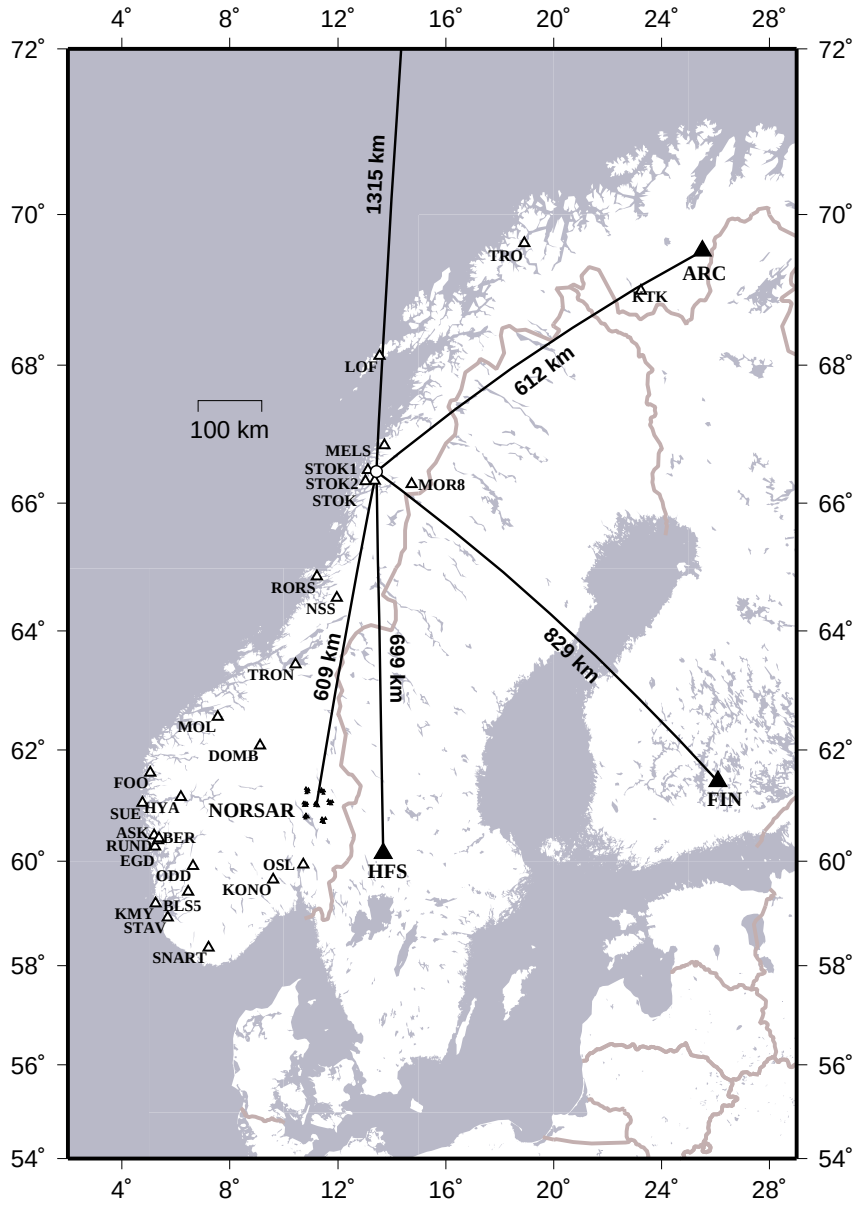


Fig. 1. Location of the 24 June, 2005, earthquake in the Rana district of Norway in relation to stations of the NNSN (white triangles) and the Fennoscandian IMS arrays (black triangles). The line leading northwards leads to the Spitsbergen array, SPI, on the island of Svalbard (designated station AS72 of the IMS).

Table 1
Events exceeding magnitude 2.0 in the Rana region during 2005 with NORSAR analyst locations based only upon phase readings from the IMS arrays displayed in Figure 1. The origin time is given in the format *yyyy-ddd:hh.mm.ss.msc* where *ddd* is the julian day. Depth is fixed to zero for all locations and magnitude estimates are provided by the GBF algorithm (Ringdal and Kværna, 1989).

| Event ID | Date | Origin time (GMT) | Latitude | Longitude | Magnitude |
|---|---|---|---|---|---|
| 7872 | Apr 28 | 2005-118:15.08.56.31 | 66.3387 | 13.8208 | 2.51 |
| 7875 | May 1 | 2005-121:07.27.30.52 | 66.2052 | 13.4615 | 2.41 |
| 8033 | Jun 24 | 2005-175:04.25.39.87 | 66.3780 | 13.6786 | 3.45 |
| 8368 | Oct 13 | 2005-286:14.08.38.88 | 66.3674 | 13.4287 | 3.09 |
| 8559 | Dec 15 | 2005-349:16.47.12.31 | 66.3384 | 13.8664 | 3.03 |

Table 2
Mean normalised correlation coefficients for 180.0 second long data segments averaged over all 42 short-period vertical channels of the NORSAR array for all event pairs from the five events listed in Table 1. Diagonal elements are all trivially equal to unity. Entries in the table above and below the diagonal are obtained in the 2.0-5.0 Hz and 3.0-8.0 Hz frequency bands respectively.

| Day of Event | Apr 28 | May 1 | Jun 24 | Oct 13 | Dec 15 |
|---|---|---|---|---|---|
| Apr 28 | 1.0 | 0.0292 | 0.7878 | 0.0267 | 0.6170 |
| May 1 | 0.0264 | 1.0 | 0.0241 | 0.0234 | 0.0263 |
| Jun 24 | 0.7249 | 0.0189 | 1.0 | 0.0233 | 0.7483 |
| Oct 13 | 0.0205 | 0.0215 | 0.0246 | 1.0 | 0.0237 |
| Dec 15 | 0.4689 | 0.0251 | 0.6569 | 0.0194 | 1.0 |

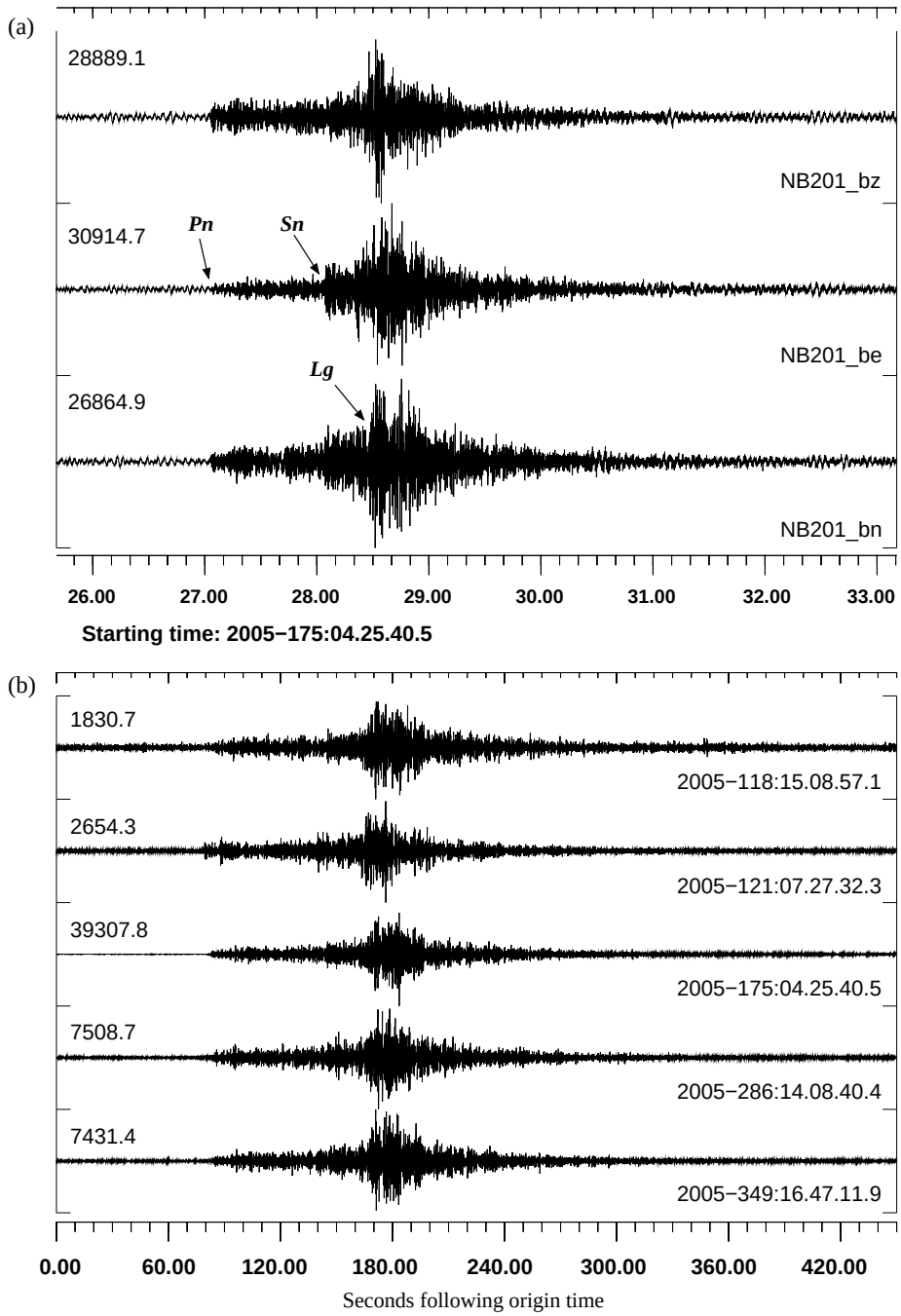


Fig. 2. Recordings at the NORSAR array of the five events listed in Table 1. Panel (a) shows unfiltered waveforms for event 8033 on the vertical, east-west and north-south components of the broadband NB201 3-component instrument. Panel (b) shows short period vertical waveforms, bandpass-filtered between 2.0 and 5.0 Hz, for all five events at the central NB200 seismometer.

Table 3
Detections made between Jan 1, 2005, and Dec 31, 2005, for a matched filter detector on the NORSAR array where the template consists of 120.0 second long data segments of waveforms bandpass filtered between 2.0 and 8.0 Hz corresponding to event with ID 8033 in Table 1. C.C. coef. is the fully-normalised array correlation coefficient and the scaling factor, $\alpha$, is the scalar multiple of the master waveform which minimises the residual when the detected waveform is subtracted (see Gibbons and Ringdal, 2006). The subsequent magnitude estimate is given by $M = \log_{10}(\alpha)+3.5$. The reference time, $t_{\mathrm{R}}$, used is 2005-175:04.25.41.000.

| Det. | Date | Julian time | C.C. coef. | Scaling factor. | mag. |
|---|---|---|---|---|---|
| 1 | Jan 25 | 025:16.47.29.719 | 0.0330 | 0.000037 | -0.93 |
| 2 | Feb 6 | 037:02.13.07.446 | 0.0740 | 0.000770 | 0.39 |
| 3 | Feb 19 | 050:04.03.00.086 | 0.1411 | 0.001730 | 0.74 |
| 4 | Mar 4 | 063:10.32.20.833 | 0.3796 | 0.007940 | 1.40 |
| 5 | Apr 6 | 096:10.54.57.970 | 0.0432 | 0.000543 | 0.23 |
| 6 | Apr 28 | 118:10.48.42.936 | 0.0662 | 0.000901 | 0.45 |
| 7 | Apr 28 | 118:15.08.57.788 | 0.7970 | 0.044560 | 2.15 |
| 8 | Apr 28 | 118:15.10.21.033 | 0.0854 | 0.004700 | 1.17 |
| 9 | Apr 28 | 118:15.14.38.837 | 0.0487 | 0.000348 | 0.04 |
| 10 | Apr 28 | 118:15.16.18.097 | 0.1267 | 0.001410 | 0.65 |
| 11 | Apr 28 | 118:15.50.02.263 | 0.0636 | 0.000672 | 0.33 |
| 12 | Apr 30 | 120:12.41.24.221 | 0.0682 | 0.000687 | 0.34 |
| 13 | May 15 | 135:03.31.10.775 | 0.0602 | 0.000461 | 0.16 |
| 14 | May 16 | 136:07.00.16.105 | 0.0534 | 0.000562 | 0.25 |
| 15 | May 19 | 139:03.58.24.572 | 0.0859 | 0.000795 | 0.40 |
| 16 | May 21 | 141:11.28.53.963 | 0.0493 | 0.000670 | 0.33 |

Table 3
continued.

| Det. | Date | Julian time | C.C. coef. | Scaling factor. | mag. |
|---|---|---|---|---|---|
| 17 | Jun 2 | 153:14.07.49.892 | 0.1846 | 0.002650 | 0.92 |
| 18 | Jun 10 | 161:15.39.30.817 | 0.2854 | 0.004390 | 1.14 |
| 19 | Jun 10 | 161:16.25.34.695 | 0.1486 | 0.002140 | 0.83 |
| 20 | Jun 10 | 161:16.39.01.043 | 0.0435 | 0.000481 | 0.18 |
| 21 | Jun 10 | 161:17.46.26.336 | 0.0309 | 0.000250 | -0.10 |
| 22 | Jun 17 | 168:00.50.55.884 | 0.0664 | 0.000645 | 0.31 |
| 23 | Jun 24 | 175:04.25.41.000 | 1.0000 | 1.000000 | 3.50 |
| 24 | Jun 24 | 175:05.02.16.254 | 0.1741 | 0.002790 | 0.95 |
| 25 | Sep 5 | 248:04.58.22.973 | 0.4419 | 0.007200 | 1.36 |
| 26 | Sep 12 | 255:23.49.03.892 | 0.0774 | 0.000747 | 0.37 |
| 27 | Sep 24 | 267:09.56.29.013 | 0.0354 | 0.000360 | 0.06 |
| 28 | Oct 19 | 292:19.40.56.155 | 0.1355 | 0.001330 | 0.62 |
| 29 | Dec 14 | 348:05.53.06.775 | 0.0577 | 0.000663 | 0.32 |
| 30 | Dec 15 | 349:16.47.13.008 | 0.7363 | 0.165670 | 2.72 |
| 31 | Dec 15 | 349:16.47.57.783 | 0.0497 | 0.010390 | 1.52 |
| 32 | Dec 31 | 365:09.54.11.126 | 0.0443 | 0.000422 | 0.13 |

Table 4
A waveform correlation detector was run on each of the Nordic IMS array stations for short time-windows surrounding each of the detections listed in Table 3. In each case, the template signal consisted of 120.0 seconds of data, bandpass filtered between 2.0 and 8.0 Hz, starting with the first predicted phase arrival where the event reference time, $t_{\mathrm{R}}$, is set to 2005-175:04.25.41.000. All waveforms were resampled to 200 Hz and a spline interpolation scheme was used to find the time of the cross-correlation beam maximum. The first time provided is the corresponding reference time, $t_0$, for each event according to correlation on the NORSAR array. The reference times for the listed arrays are given by $t_0 \ + \delta t$. rARC denotes a reduced ARCES array consisting of only the innermost 9 elements. A dash indicates non-detection.

| Det. | $t_0$: NORSAR | $\delta t$: ARC | $\delta t$: rARC | $\delta t$: HFS | $\delta t$: FIN | $\delta t$: SPI |
|---|---|---|---|---|---|---|
| 1 | 025:16.47.29.71983 | - | - | - | - | - |
| 2 | 037:02.13.07.44567 | 0.0809 | 0.0791 | -0.0034 | 0.0053 | - |
| 3 | 050:04.03.00.08567 | 0.1421 | 0.1421 | 0.0116 | 0.0919 | - |
| 4 | 063:10.32.20.83350 | 0.0635 | 0.0639 | 0.0044 | 0.0411 | - |
| 5 | 096:10.54.57.96950 | No data | No data | - | - | - |
| 6 | 118:10.48.42.93517 | 0.0490 | 0.0490 | -0.0060 | - | - |
| 7 | 118:15.08.57.78750 | 0.0325 | 0.0333 | 0.0046 | 0.0255 | 0.0242 |
| 8 | 118:15.10.21.03167 | 0.0051 | 0.0063 | 0.0010 | - | - |
| 9 | 118:15.14.38.83600 | 0.0316 | 0.0294 | 0.4601 | - | - |
| 10 | 118:15.16.18.09733 | 0.0615 | 0.0623 | 0.0062 | 0.0519 | - |
| 11 | 118:15.50.02.26317 | 0.0608 | 0.0594 | 0.0093 | - | - |
| 12 | 120:12.41.24.22050 | 0.0401 | 0.0389 | 0.0045 | - | - |
| 13 | 135:03.31.10.77600 | 0.0250 | - | 0.0084 | - | - |
| 14 | 136:07.00.16.10533 | -0.0099 | -0.0133 | - | - | - |
| 15 | 139:03.58.24.57183 | 0.0304 | 0.0326 | 0.0101 | - | - |
| 16 | 141:11.28.53.96217 | 0.0062 | 0.0048 | - | - | - |

Table 4
continued.

| Det. | $t_0$: NORSAR | $\delta t$: ARC | $\delta t$: rARC | $\delta t$: HFS | $\delta t$: FIN | $\delta t$: SPI |
|---|---|---|---|---|---|---|
| 17 | 153:14.07.49.89133 | 0.0317 | 0.0325 | 0.0041 | 0.0219 | - |
| 18 | 161:15.39.30.81667 | -0.0145 | -0.0129 | 0.0009 | -0.0081 | - |
| 19 | 161:16.25.34.69450 | -0.0217 | -0.0203 | -0.0002 | -0.0129 | - |
| 20 | 161:16.39.01.04267 | -0.0303 | -0.0279 | - | - | - |
| 21 | 161:17.46.26.33400 | -0.0242 | - | - | - | - |
| 22 | 168:00.50.55.88450 | 0.0231 | 0.0225 | - | 0.0153 | - |
| 23 | 175:04.25.41.00000 | 0.0000 | 0.0000 | 0.0000 | 0.0000 | 0.0000 |
| 24 | 175:05.02.16.25400 | -0.0314 | -0.0308 | -0.0001 | -0.0274 | - |
| 25 | 248:04.58.22.97267 | -0.0243 | -0.0229 | -0.0015 | -0.0189 | - |
| 26 | 255:23.49.03.89300 | -0.0500 | -0.0466 | -0.0045 | -0.0172 | - |
| 27 | 267:09.56.29.01283 | -0.0674 | - | - | - | - |
| 28 | 292:19.40.56.15483 | 0.0224 | 0.0248 | -0.0008 | - | - |
| 29 | 348:05.53.06.77517 | -0.0518 | -0.0514 | -0.0165 | - | - |
| 30 | 349:16.47.13.00883 | -0.0582 | -0.0570 | -0.0017 | -0.0344 | -0.0390 |
| 31 | 349:16.47.57.78367 | 0.0049 | - | -0.0123 | - | - |
| 32 | 365:09.54.11.12583 | -0.2224 | -0.2196 | - | - | - |

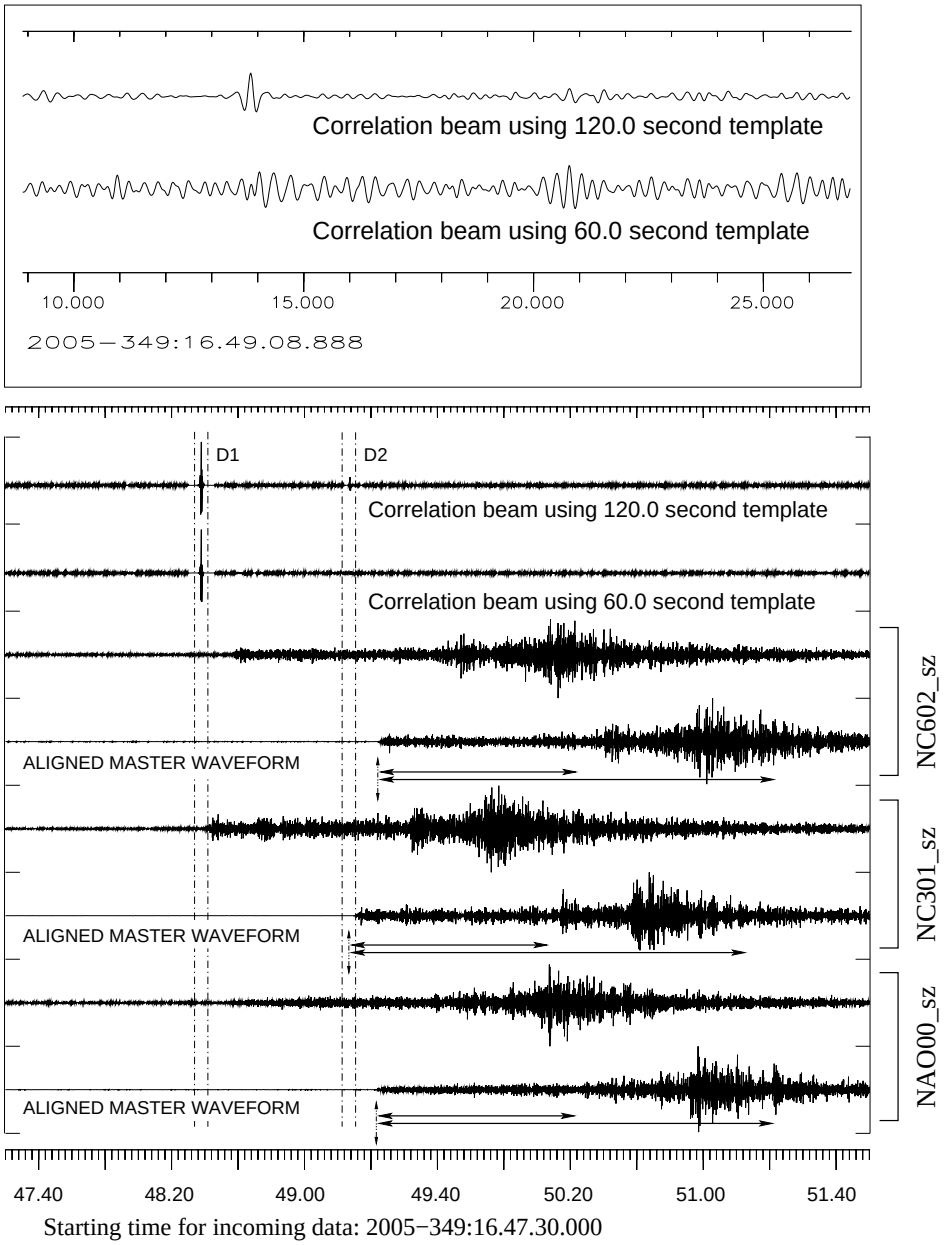


Fig. 3. Detection using the NORSAR array of a presumed aftershock to the main event on December 15, 2005, using the June 24 main event signal as a template. D1 and D2 correspond to detections 30 and 31 in Table 3. Incoming data is shown for three channels as indicated together with the corresponding segments from the master event, aligned according to the time of detection D2. Note how the master waveform segments are staggered according to the *Pn* arrivals. The correlation coefficient beams are displayed for the cases of 60.0 and 120.0 second long waveform templates and it is clear (see inset panel for details) that the very marginal detection 31 (D2) is not made when only the shorter data segment is used. The actual segments of data corresponding to the two window lengths are indicated by arrows below the master waveform segments.

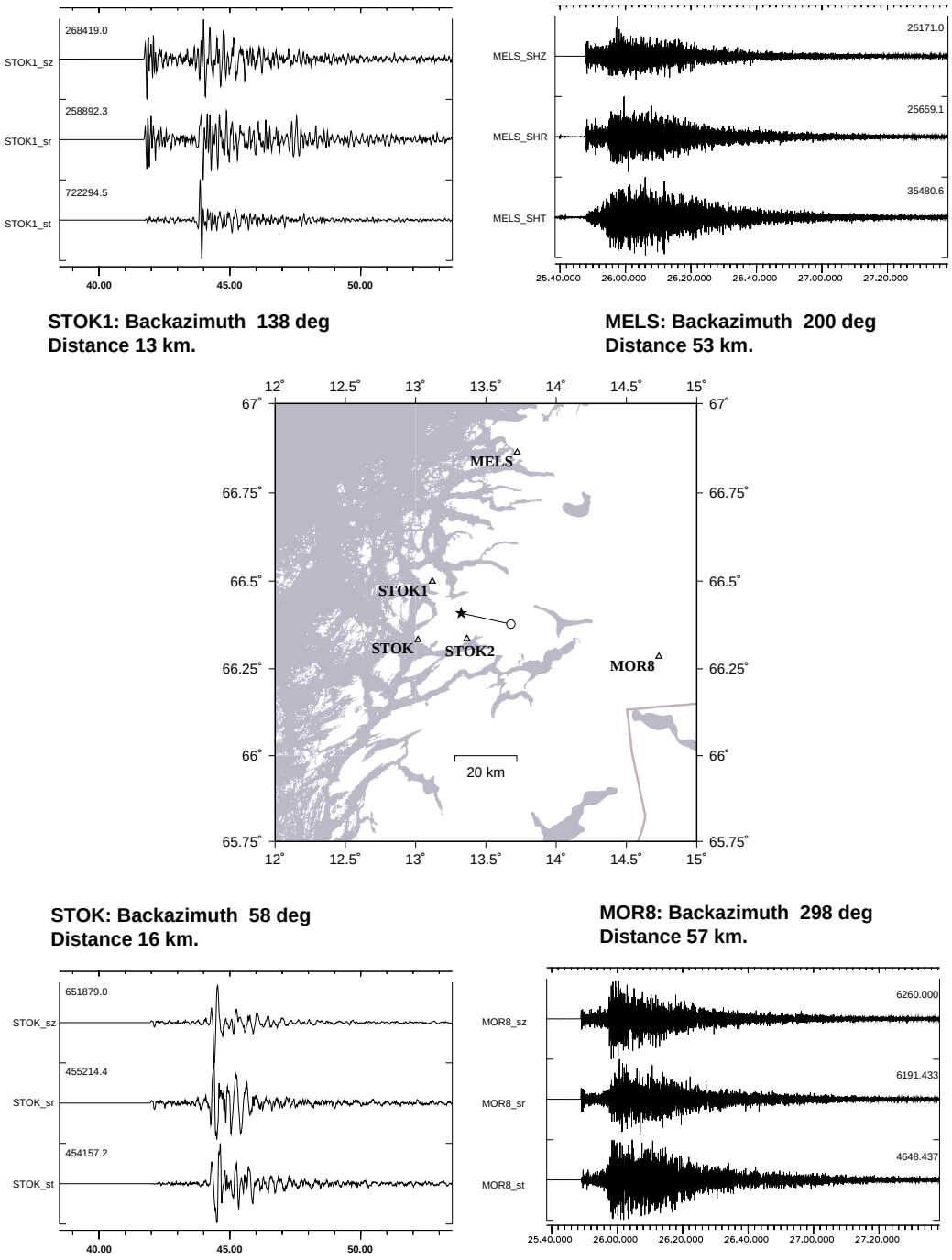


Fig. 4. Location estimates for the June 24, 2005, event. The white circle denotes the location indicated in Table 1 and the black star indicates a new estimate based upon P- and S- picks from the four stations displayed: MELS (Meløy), STOK (Stokkvågen), STOK1 (temporary installation) and MOR8 (Mo i Rana). The temporary STOK2 station was not in operation at the time of this event. All waveforms are unfiltered, seismograms all begin at the origin time estimate 2005-175:04.25.38.485, and all horizontal components are rotated according to the backazimuths indicated.

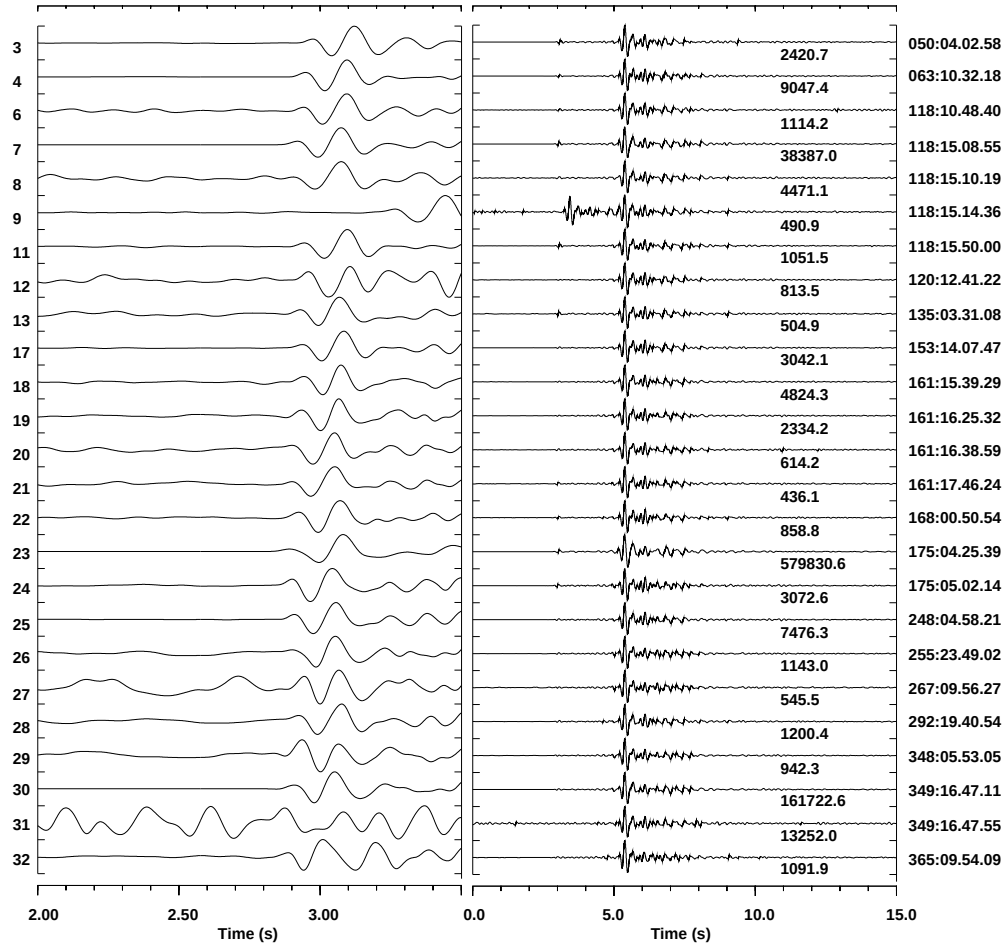


Fig. 5. Waveforms recorded at the STOK station for the times corresponding to the NORSAR correlation detections as listed in Table 3. The right panel displays a 15.0 second long data segment from the short period vertical channel with each waveform aligned to provide maximum correlation with a 2.0 second long window containing the S-arrival for the the June 24 main event. The left panel displays a 1.5 second long segment containing the far lower amplitude P-arrival for each event with exactly the same alignment as displayed in the right panel. Observed differences in the P-arrival are indications of S minus P travel time differences for this station. Numbers missing from the left hand side indicate detections in Table 3 for which no STOK data exists. All waveforms are bandpass filtered between 2.0 and 8.0 Hz.

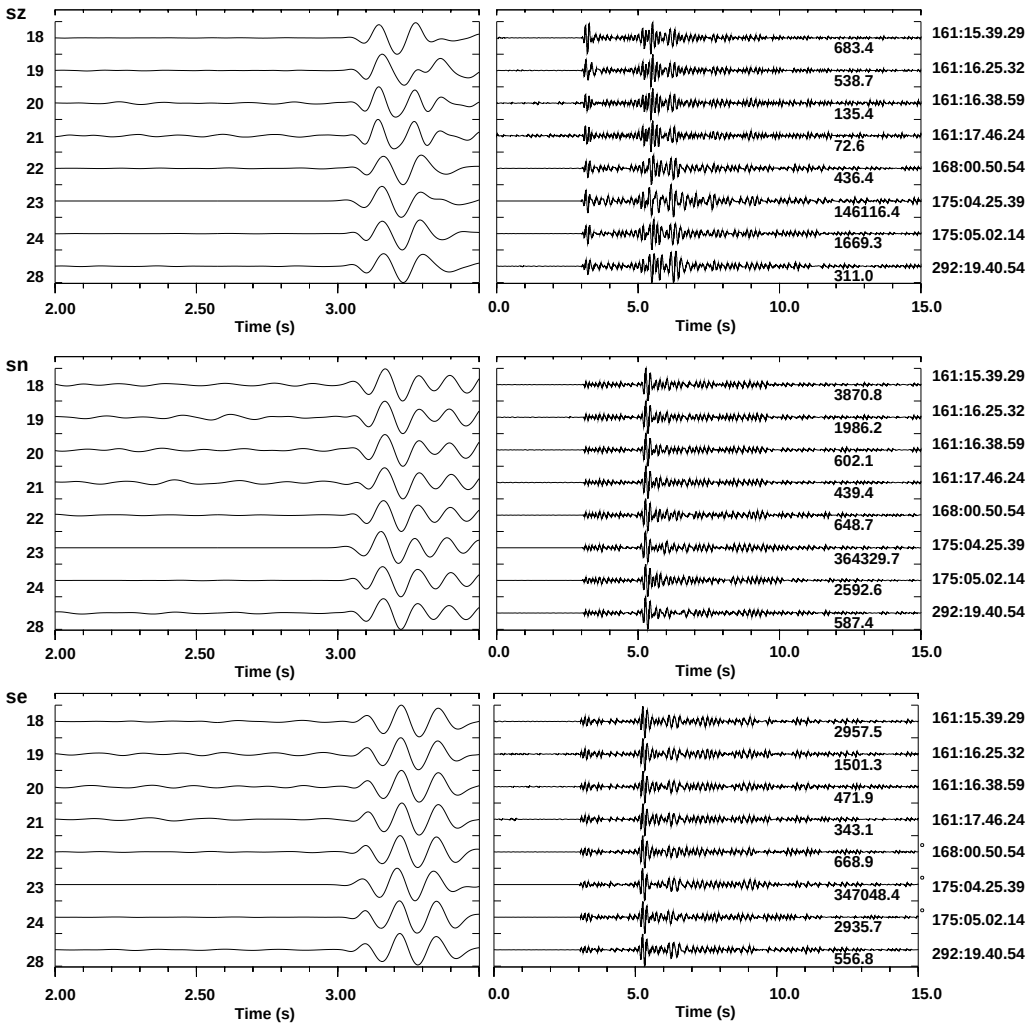


Fig. 6. Waveforms recorded at the STOK1 station for the times corresponding to the NORSAR correlation detections as listed in Table 3. sz, sn and se denote the short period vertical, North-South and East-West components respectively. Alignment in both left and right panels is based upon a maximum correlation with a 3.0 second time-window of the June 24 main event starting at the S-arrival.

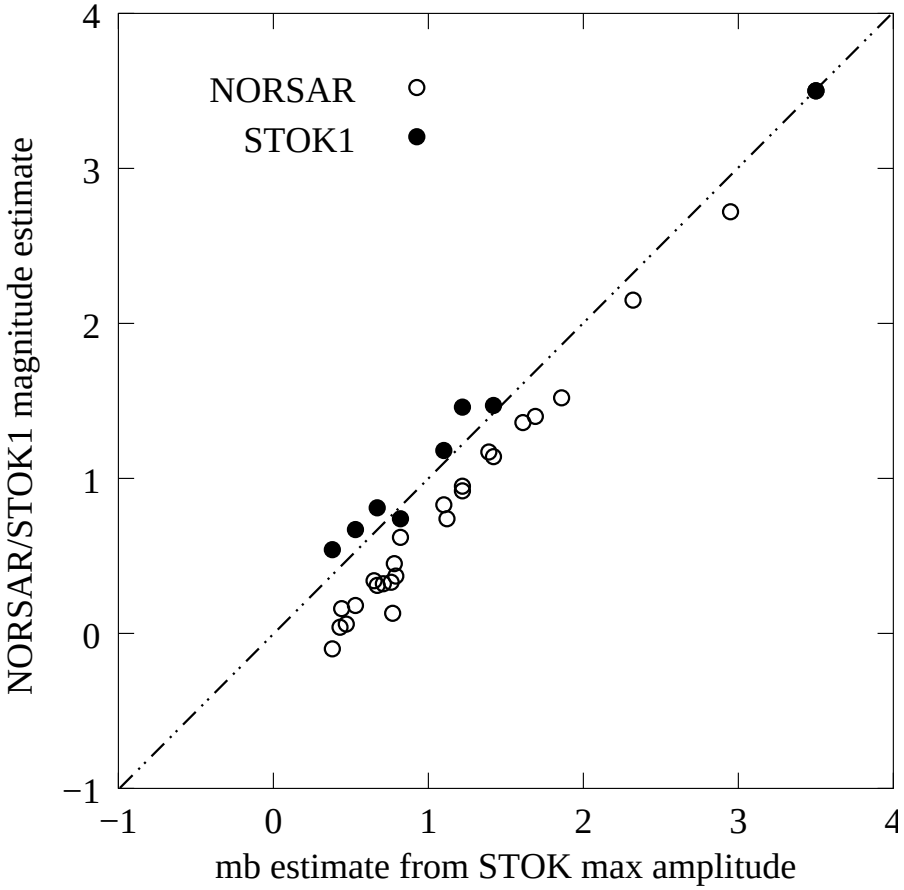


Fig. 7. Comparison of magnitudes estimated using maximum amplitudes at the STOK station (see Figure 5) and those obtained using independent measurements on amplitudes at the temporary STOK1 station (see Figure 6) and correlation and least squares inversion at the NORSAR array (described by Gibbons and Ringdal (2006) and listed in Table 3). The magnitude of the main June 24 event is fixed to 3.50.

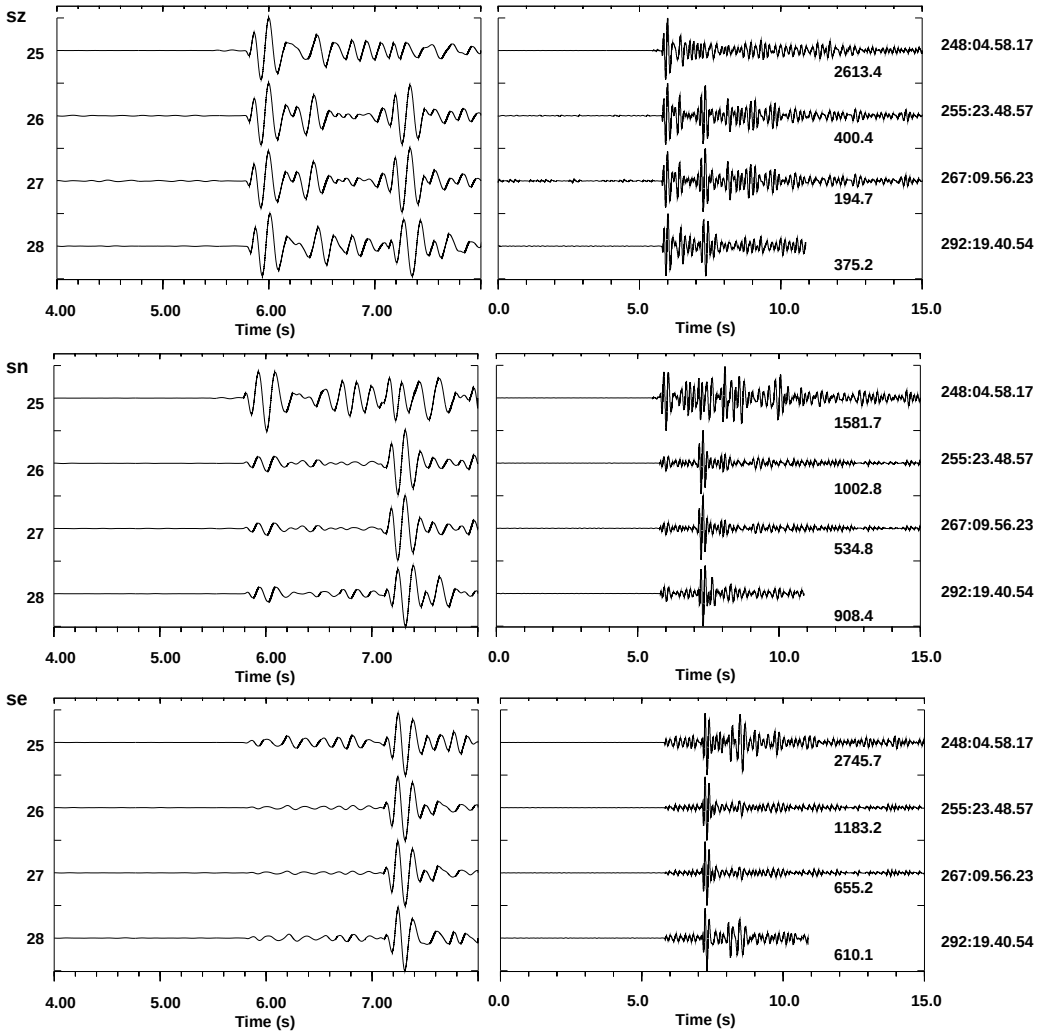


Fig. 8. Waveforms recorded at the STOK2 station for the times corresponding to the NORSAR correlation detections as listed in Table 3. sz, sn and se denote the short period vertical, North-South and East-West components respectively. Alignment in both left and right panels is based upon a maximum correlation with a 1.4 second time-window of the September 24 event starting at the P-arrival.

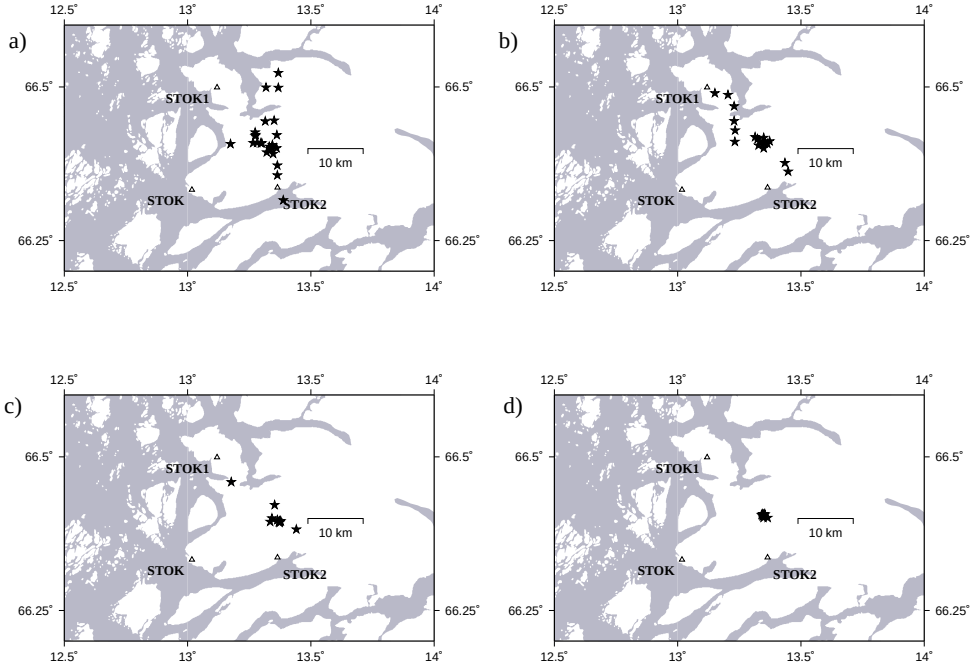


Fig. 9. Location estimates for the event set. (a) shows preliminary event-by-event locations using the HYPOSAT program using all available manual arrival picks and P-phase polarisation azimuth estimates from the local stations (including MOR8 and MELS). (b) shows a double-difference (DD) relocation of these events using the locations from (a) as an initial condition. (c) shows DD relocations using a single source initial location estimate of 66.4039°N, 13.3489°E, depth 12.0km and (d) shows the results of the same calculation but with the initial depth fixed to 0.0. Many events were deleted at various iterations of the DD relocation procedure; panels a), b), c) and d) display location estimates for 25, 18, 14 and 11 events respectively.

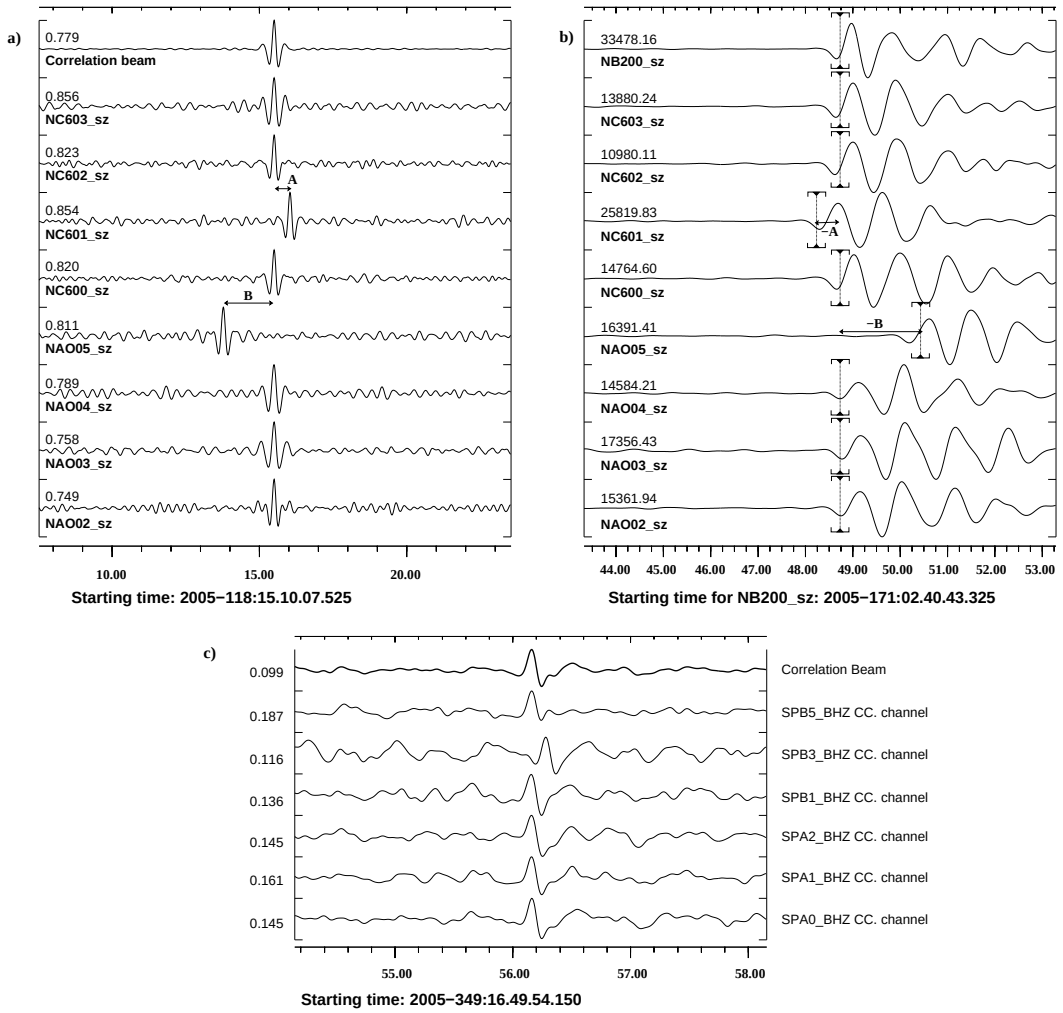


Fig. 10. Exploitation of repeating seismic events for the identification and measurement of timing discrepancies between sites of an array or network. (a) displays correlation coefficient traces for 8 of the 42 short period vertical channels of the NORSAR array (together with the correlation beam) for a 15 second long time-segment on April 28, 2005, where the master signal template consists of 120.0 second long data segments extracted from the main 24 June 2005 event, filtered between 2.0 and 12.0 Hz. To within the time resolution available, all channels achieve a maximum correlation coefficient simultaneously except for sites NC601 and NAO05; these differ from the common correlation time by delays labelled A and B respectively. (b) shows a P-arrival from a large teleseismic event on 21 June 2005 (origin time according to United States Geological Survey 02.32.59.97: latitude 36.35°, longitude 71.08°, depth 235km, $m_b$ = 5.2; see http://neic.usgs.gov/neis/epic/epic_rect.html) which reaches the NB200 central element at a time 2005-171:02.40.47.875. The remaining channels are delayed according to the best-fit, uncorrected, plane wavefront and the markers indicate the relative times deduced from the maximum correlation times in (a). Waveforms are bandpass-filtered between 0.8 and 2.0 Hz. (c) shows aligned correlation coefficient channels on the SPITS array using the June 24 Mo i Rana event as a master signal. SPB3 is clearly anomalous by a fraction of a second.